MJFAS
Malaysian Journal of Fundamental and Applied Sciences

Lestari *et al.* | Malaysian Journal of Fundamental and Applied Sciences, Vol. 22 (2026) 654-669

RESEARCH ARTICLE

Eco-Friendly Synthesis of Silver Nanoparticles Using *Plumeria acuminata L.* for Colorimetric Detection of Pb^{2+} in Lipstick Samples

Gusti Ayu Dewi Lestari[a,*], I Gusti Agus Surya Pratama Saputra[a], Pande Koming Agnesya Wulan Devi[a], Si Ayu Dian Natalia[a], Aliya Nur Hasanah[bc]

[a]Department of Pharmacy, Faculty of Pharmacy and Health Sciences, Universitas Pendidikan Nasional, 80224, Bali, Indonesia; [b]Department of Pharmaceutical Analysis and Medicinal Chemistry, Faculty of Pharmacy, Universitas Padjadjaran, Jl. Raya Bandung Sumedang KM 21.5, Sumedang 45363, Indonesia; [c]Drug Development Study Center, Faculty of Pharmacy, Universitas Padjadjaran, Jl. Raya Bandung Sumedang KM 21.5, Sumedang 45363, Indonesia

Abstract Exposure to heavy metals such as lead (Pb) in cosmetic products is a concern because it can cause toxic health effects with long-term use. This study aims to synthesize silver nanoparticles (AgNPs) using a green synthesis method from the waste extract of frangipani leaves (*Plumeria acuminata* L.) and evaluate their potential as biosensors for Pb detection in lipstick samples. The formation of AgNPs is characterized by a change in the solution's color to reddish-brown and confirmed by UV–Vis analysis, which shows a maximum absorption peak at 408 nm due to the surface plasmon resonance (SPR) phenomenon. PSA results show an average particle size of 57.28 nm, a PDI of 0.3254, and a zeta potential of −25.53 mV. XRD and TEM analyses show that AgNPs have a face-centered cubic (FCC) crystal structure, a size of 21.98 nm, and a spherical shape. The selectivity test results show that AgNPs exhibit a stronger response to Pb metal than to other metals. Analytical performance evaluation showed good linearity with a regression equation of y = -0.0034x + 0.5377 and R^2 value of 0.9922. The developed method also showed good accuracy and precision, with a recovery of 98.69-107.03% and %RSD of 3.01%, as well as LOD and LOQ values of 3.17 ppm and 9.59 ppm, respectively. Tests on authentic lipstick cosmetic samples showed that no Pb^{2+} response was detected under the experimental conditions. Overall, the green-synthesized AgNPs have the potential to serve as a simple, environmentally friendly colorimetric biosensor for detecting Pb in cosmetic products.

Keywords: AgNPs; colorimetric biosensor; green synthesis; Pb detection; *Plumeria acuminata* L.

***For correspondence:**
dewilestari@undiknas.ac.id

Received: 14 May 2026
Accepted: 24 June 2026

Introduction

The increasing use of cosmetic products has paralleled the growing public awareness of personal care and physical appearance. Despite their widespread use, cosmetic safety remains a critical public health concern, particularly due to contamination with toxic heavy metals such as lead (Pb), cadmium (Cd), and chromium (Cr). Since cosmetics are routinely applied directly to the skin, lips, and other sensitive body surfaces, prolonged exposure may facilitate dermal absorption and contribute to chronic accumulation of toxic elements in the human body. Consequently, the presence of heavy metals in cosmetic products has become an important issue requiring continuous monitoring and regulatory oversight [1]. Reports issued by the Indonesian Food and Drug Monitoring Agency (BPOM) have identified cosmetic products containing prohibited substances, including lead, indicating that heavy metal contamination continues to pose a challenge to cosmetic safety management [2].

Among cosmetic products, lipstick is one of the most frequently used and consists of a complex mixture of pigments, waxes, oils, and various additives. During manufacturing, contamination by heavy metals may occur through raw materials, pigments, processing equipment, or production environments. Lead contamination is particularly concerning because lipstick is applied directly to the lips and may be inadvertently ingested during routine use. Continuous exposure to lead-contaminated lipstick may therefore contribute to cumulative lead intake and subsequent adverse health effects [3]. Several studies have reported detectable levels of lead in both registered and unregistered lipstick products available on the market, raising concerns regarding long-term consumer safety [4,5]. Lead is a persistent environmental pollutant that is resistant to degradation and readily accumulates in biological systems and food chains [6]. Chronic lead exposure has been associated with numerous adverse health outcomes, including neurotoxicity, cognitive impairment, anemia, hypertension, nephrotoxicity, and reproductive disorders. The World Health Organization (WHO) has emphasized that no level of lead exposure can be considered completely safe, and blood lead concentrations as low as 3.5 µg/dL have been linked to significant health consequences [7].

To monitor lead contamination, several highly sensitive analytical techniques have been developed, including Atomic Absorption Spectrometry (AAS), Inductively Coupled Plasma Mass Spectrometry (ICP-MS), Inductively Coupled Plasma Optical Emission Spectrometry (ICP-OES), Atomic Fluorescence Spectrometry (AFS), and Laser-Induced Breakdown Spectrometry (LIBS) [8]. Although these methods provide excellent sensitivity and accuracy, their implementation is often constrained by expensive instrumentation, labor-intensive sample preparation, the need for skilled personnel, and limited suitability for rapid on-site analysis [8–10]. Therefore, there is an increasing demand for simple, rapid, cost-effective, and portable analytical approaches for routine lead detection.

Recent advances in nanotechnology have promoted the development of silver nanoparticles (AgNPs) as highly promising colorimetric sensing materials. AgNPs exhibit unique optical properties arising from localized surface plasmon resonance (SPR), which is highly sensitive to changes in the surrounding environment. Interactions between AgNPs and metal ions can induce particle aggregation or surface modifications, resulting in distinct color changes that can be observed visually or monitored spectroscopically. These characteristics make AgNPs-based colorimetric sensors attractive due to their simplicity, rapid response, low operational cost, and high sensitivity [12]. Nevertheless, conventional synthesis of AgNPs frequently employs chemical reducing agents such as sodium borohydride ($NaBH_4$), which are associated with toxicity and environmental concerns [13]. To overcome these limitations, environmentally benign green synthesis approaches have been developed using plant-derived biomolecules as both reducing and stabilizing agents [14].

Frangipani (*Plumeria acuminata* L.) is an abundant ornamental plant widely distributed throughout Bali, Indonesia, and represents a potentially valuable source of renewable biomaterials [15]. In particular, fallen frangipani leaves constitute an underutilized biomass waste despite containing diverse phytochemicals, including flavonoids, phenolic compounds, tannins, alkaloids, terpenoids, and glycosides, which can facilitate nanoparticle synthesis [16]. Reported constituents of *P. acuminata* include agoniadin, plumeric acid, lupeol, serotinic acid, plumieride, flavonoids, polyphenols, and volatile compounds such as geraniol, farnesol, eugenol, citronellol, phenethyl alcohol, and linalool [17, 18]. These biomolecules possess abundant hydroxyl and other electron-rich functional groups that can donate electrons during nanoparticle formation. Mechanistically, phenolic hydroxyl groups undergo oxidation to quinone-like structures, releasing electrons that reduce silver ions (Ag^+) into metallic silver (Ag^0). Simultaneously, the oxidized organic molecules adsorb onto the nanoparticle surface, functioning as capping agents that provide steric stabilization and inhibit particle aggregation, thereby enhancing colloidal stability and nanoparticle dispersion [19, 20].

Although green synthesis of AgNPs using plant extracts has been extensively investigated, most studies have focused on antibacterial, antimicrobial, and biomedical applications [16, 21]. More recently, AgNPs have attracted considerable attention as colorimetric biosensors for heavy metal detection due to their highly sensitive optical responses to target analytes [12]. Several studies have demonstrated the feasibility of using agricultural biomass waste for AgNPs synthesis and metal-ion sensing. For example, orange peel-mediated AgNPs have been successfully applied for the detection of Pb^{2+} and Cd^{2+} ions through characteristic UV–Vis spectral changes [22]. At the same time, coffee peel-derived AgNPs have been employed for mercury ion detection in cosmetic samples [23]. Despite these promising developments, the use of frangipani leaf waste as a bioreductant for AgNPs synthesis and its application in Pb^{2+} detection remains largely unexplored. Furthermore, a significant gap persists in the availability of rapid, low-cost, and decentralized analytical methods suitable for routine screening of heavy metals in cosmetic products. Therefore, this study aims to synthesize biogenic silver nanoparticles using waste leaves of *Plumeria acuminata* L. and evaluate their potential as a colorimetric sensor for Pb^{2+} detection

in lipstick samples. The proposed approach offers an environmentally sustainable and economically viable alternative to conventional analytical techniques while supporting the development of accessible monitoring tools for cosmetic safety assessment.

Materials and Methods

The Material used in this research were Silver Nitrate $AgNO_3$, Ca^{2+}, K^+, Zn^{2+}, Mg^{2+}, HNO_3 (ROFA), Pb^{2+}, Na^+ (Pudak Scientific), HCl (Merck), *Plumeria* leaves waste (*Plumeria acuminata* L.), demineralized water (ROFA) Lipstick samples (online market), UV-Vis Spectrophotometer (Genesys), cuvette (TRIDILAB), Water bath (Memmer), XRD (Bruker D8 Advance), TEM (Hitachi HT7700), and PSA (Zetasizer Advance Pro Blue Malvern), vial bottle (ROFA), Blender (Philips), Erlenmeyer flask (Iwaki), measuring cylinder (Herma), beaker glass (Iwaki), oven (OV-30), sonicator (GT Sonic), volumetric flask (Pyrex), Hot plate (MASPION).

Preparation of Plant Extract

Fallen and wilted frangipani (*Plumeria acuminata* L.) leaf waste was collected from the Banjar Guliang Kawan area, Bunutin Village, Bangli, Bali. The yellowed leaf waste was collected, then dried in an oven at 50°C and blended to form a powder. A total of 0.5 g of frangipani leaf simplicia was weighed and dissolved in 100 mL of demineralized water, then sonicated for 30 minutes at 50°C, and then filtered to obtain the extract.

Green Synthesis of AgNPs Using Leaf Extract

AgNPs synthesis was carried out by mixing a 1 mM $AgNO_3$ solution with frangipani leaf extract. The volume ratio between frangipani leaf extract and $AgNO_3$ solution was 1:9 (v/v), adjusted to pH 11 with 0.1 N NaOH, then homogenized and left at room temperature. Alkaline environments induce the deprotonation of functional groups (such as hydroxyl, carboxyl, and amino groups) present in the biomolecules or capping agents within the reaction mixture and drastically boosting their reducing capability and accelerating the reduction potential of silver ions. As an indicator of the formation of AgNPs, it was visually indicated by a color change from clear yellow to reddish brown [20]. The synthesized AgNPs colloidal solution was stored in a brown glass bottle at room temperature. Under these conditions, the particles remained stable without significant aggregation for up to 6 months.

Characterization of AgNPs

Characterization of AgNPs was carried out using a UV-Vis spectrophotometer to confirm the formation of AgNPs through observation of the surface plasmon resonance (SPR) absorption peak with measurements in the wavelength range of 300-800 nm [24]. Transmission electron microscopy (TEM) aims to determine the shape and morphology of the formed nanoparticles in more detail. Samples were analyzed using a TEM instrument to obtain high-resolution images of nanoparticles. Characterization testing using X-ray diffraction (XRD) aims to determine the crystal structure and size of the AgNPs formed. AgNPs samples were analyzed at an angle range of 2θ between 20° and 90° to obtain diffraction patterns [24]. Characterization using a particle size analyzer (PSA) aims to determine the size, particle size distribution in solution, and the zeta potential of AgNPs. Nanoparticles generally have a size in the range of 1–100 nm [25].

Pb^{2+} Detection Using AgNPs

It was done by preparing a Pb stock solution with a concentration of 100 ppm, then making variations in concentration in the range of 25-50 ppm. Each concentration was reacted with 0.2 mL of AgNPs, and each concentration was diluted with water until a total volume of 4 mL was obtained. The mixture was homogenized and incubated in a water bath at a temperature of 50°C for 10 minutes. The test was carried out with a UV-Vis spectrophotometer at a wavelength of 200-800 nm. Absorbance measurements were carried out to obtain analytical responses related to Pb concentration, where changes in absorbance were related to the interaction between the metal and AgNPs [10]. The obtained absorbance values were plotted to produce a calibration curve and a linear regression equation. Analytical parameters such as correlation coefficient (r), limit of detection (LOD) and limit of quantification (LOQ) were calculated based on the slope of the curve and the standard deviation of the response [26]. Precision tests were carried out through repeated measurements of 8 replications, and accuracy tests were evaluated based on repeated measurements and the calculation of the average value of the average measurement results.

Selectivity Study of AgNPs Toward Pb^{2+}

A selectivity test was conducted to determine the response of AgNPs to Pb compared to other metals such as Na^+, Ca^{2+}, K^+, Zn^{2+}, and Mg^{2+}, with a concentration of 100 ppm. As much as 0.2 mL of AgNPs was mixed with 1 mL of each metal solution and then diluted with water to a total volume of 4 mL. The solution was analyzed visually and using a UV-Vis spectrophotometer in the range of 200-800 nm. Selectivity was determined based on differences in color changes, absorbance, and maximum wavelength shifts [9, 27].

Pb^{2+} Detection in Lipstick Sample Using Colorimetric Method

To evaluate the practical applicability of the developed colorimetric sensing method, four unbranded commercial lipstick samples with different color shades (coral red, beige, pink, and peach) were randomly purchased from a local market. These blind samples were selected to represent real-world consumer products, for which no prior information regarding brand identity, formulation, or heavy metal content was available. Approximately 1 g of each lipstick sample was accurately weighed into a beaker and digested with 12 mL of freshly prepared aqua regia (HNO_3 : HCl 1:3 v/v). The mixture was heated until the evolution of brown fumes ceased, indicating complete digestion of the organic matrix. After cooling to room temperature, the solution was filtered through Whatman filter paper to obtain a clear filtrate. The filtrate was subsequently diluted with deionized water and neutralized to pH 6–7 by the dropwise addition of 1 N NaOH, following a previously reported procedure [4].

For Pb^{2+} detection, 0.2 mL of the AgNPs was transferred into a test tube, followed by the addition of 1 mL of the prepared lipstick sample solution. The final volume was adjusted to 4 mL using demineralized water. The resulting mixture was thoroughly homogenized and incubated at 50 °C for 10 min to facilitate interaction between Pb^{2+} ions and the AgNPs. Changes in color and optical properties were subsequently evaluated using UV–Vis spectrophotometry over a wavelength range of 200–800 nm. Particular attention was given to variations in the surface plasmon resonance (SPR) band and the maximum absorbance wavelength (λmax) of the AgNPs, which served as indicators of Pb^{2+}-induced nanoparticle aggregation and detection performance.

Results and Discussion

This results and discussion section presents the synthesis of AgNPs through a green synthesis method using waste extract of frangipani leaves (*Plumeria acuminata* L.), as well as its characterization and application as a biosensor for Pb metal in cosmetic samples. Characterization includes visual observation, UV–Vis spectrophotometry, TEM, XRD and PSA to assess the physicochemical properties of nanoparticles. The UV–Vis spectrum shows a typical SPR peak that proves the formation of nanoparticles. At the same time, TEM, PSA and XRD provide data on the morphology, particle size distribution and crystalline size of AgNPs. Furthermore, AgNPs were tested as a colorimetric sensor for Pb^{2+} ion detection through selectivity testing and optical response measurements. The final results were analyzed to correlate the characteristics of nanoparticles with their performance in detecting Pb^{2+} ions.

The phytochemical screening of *Plumeria acuminata* L. extract revealed the distinct presence of flavonoids and saponins. This chemical profile is strongly corroborated by previous studies investigating the secondary metabolic composition of this species. For instance, [28] identified that the leaves and flowers of *P. acuminata* are rich sources of flavonoids and saponins, which actively contribute to its targeted biological activities. While some literature reports broader profiles that include tannins or alkaloids, our exclusive detection of flavonoids and saponins may be attributed to the specific choice of extraction solvent, plant maturity, or localized microclimatic factors unique to our sample, which heavily govern the yield and detectability of Apocynaceae metabolites

Visual Observation of AgNPs Formation

The formation of AgNPs was visually observed through the color change of the solution during the synthesis process. As seen in Figure 1, the initial $AgNO_3$ solution appeared clear and colorless, indicating that the silver ions (Ag^+) were still in dissolved form. Frangipani leaf extract with a concentration of (0.5%) had a brownish-yellow color. After the green synthesis process, the solution changed color to reddish brown, indicating the formation of AgNPs [9, 27]. The color change occurred due to the surface plasmon resonance (SPR) phenomenon, namely, the collective oscillation of electrons on the surface of metal nanoparticles when interacting with light. This color change also indicates the reduction of Ag^+ ions to Ag^0 by bioactive compounds in plant leaf extracts [29]. The reddish-brown color is a characteristic of the formation of AgNPs that has been widely reported in green synthesis methods. Bioactive compounds in plant

extracts, such as flavonoids and phenolics, act as reducing agents as well as stabilizers in the AgNPs synthesis process [30].

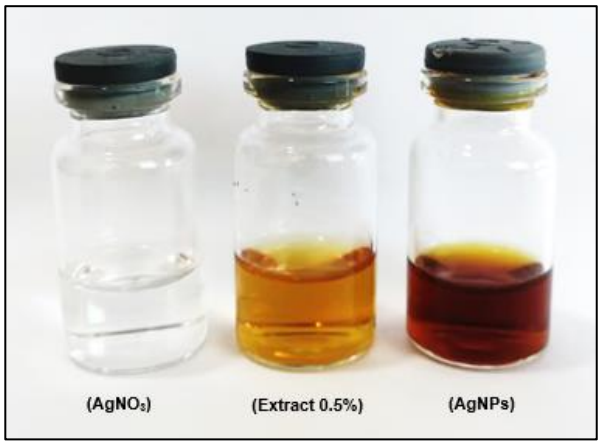

Figure 1. Visual observation of AgNPs formation: $AgNO_3$ solution, *Plumeria* leaf extract 0.5% and green-synthesized AgNPs showing colour changes.

UV-Vis Characterization of AgNPs

Characterization of AgNPs using a UV-Vis spectrophotometer was carried out to confirm the formation of nanoparticles by observing the typical absorption peak in the visible spectrum region. The measurements were performed over a wavelength range of 300-800 nm and a resolution of 1 nm. Samples were placed in a quartz cuvette, using demineralized water as the blank reference. Based on the results of the UV-Vis spectrum, it shows a maximum absorption peak (λmax) at a wavelength of 408 nm. AgNPs are known to have a typical absorption band due to the SPR phenomenon, where AgNPs generally have an absorption peak in the range of 400-500 nm, so they can be used to confirm the formation of nanoparticles through a UV-Vis spectrophotometer [10]. The SPR peak of AgNPs appears in this range as a result of plasmons on the surface of metal nanoparticles. Several studies, one of which by [31], stated that the absorption peak in the range of 400-450 indicates the formation of AgNPs. Thus, the absorption peak obtained at 408 nm in this study is in the typical SPR range of AgNPs, thus confirming the formation of AgNPs. In addition, this wavelength value also indicates that the size of the AgNPs is on the appropriate nanoscale, because the position of the SPR peak is known to be influenced by the size and morphology of the particles. The shift in wavelength towards a larger direction (red shift) is related to an increase in particle size or the presence of interactions between particles [32].

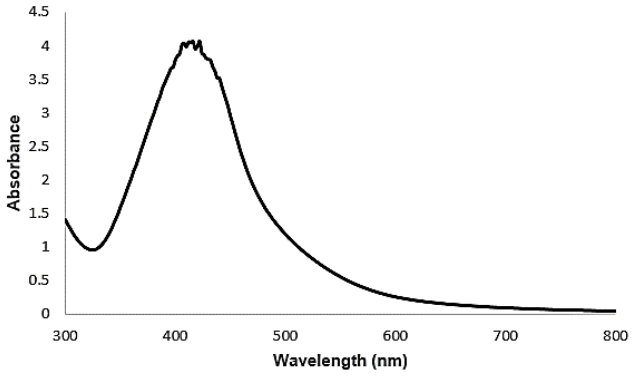

Figure 2. UV–Vis spectrum of green-synthesized AgNPs exhibiting a characteristic surface plasmon resonance (SPR) peak at 408 nm, confirming nanoparticle formation.

Particle Size and Morphology Analysis (PSA and TEM)

Transmission Electron Microscope operating at an accelerating voltage of 120 kV. Samples were prepared by dropping a diluted colloid onto a carbon-coated copper grid and allowing it to dry completely at room temperature before imaging. Magnifications ranging from 50,000x to 200,000x utilized to capture

clear structural details. The characterization results using transmission electron microscopy (TEM) in Figure 3 show that the green-synthesized AgNPs have a dominant spherical morphology. The dominant spherical shape indicates that the reduction process of Ag^{+} to Ag^{0} took place well during the synthesis using frangipani leaf extract, where compounds such as flavonoids and phenolics act as reducing agents and stabilizers (capping agents) [33]. The observed size variations are likely caused by the nucleation and growth processes of particles as well as interactions between particles [34]. These results are in accordance with previous studies that reported that green-synthesized AgNPs are generally spherical with varying size distributions [16, 35]. In addition, TEM is an effective technique for observing the morphology and size of nanoparticles directly at the nanometer scale [36].

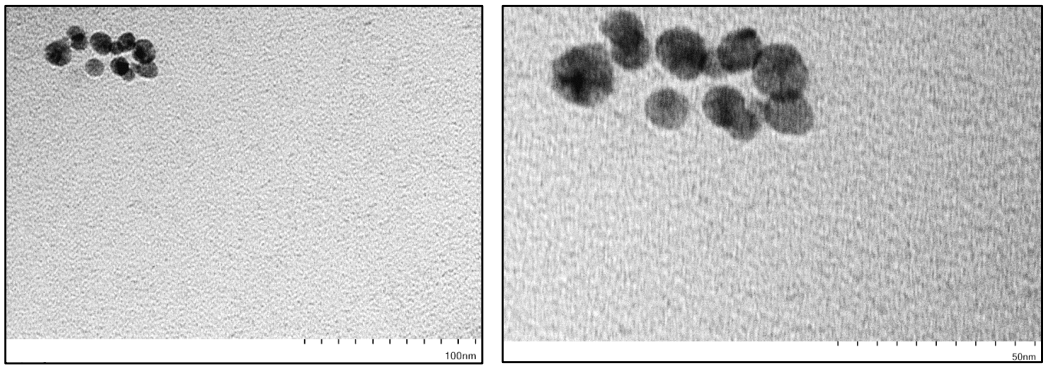

(a) (b)

Figure 3. Transmission Electron Microscopy (TEM) image of AgNPs synthesized using *Plumeria* leaf extract at different magnification (x80,000 (a) and x200,000 (b))

PSA analysis was conducted at a controlled temperature of 25°C and a fixed scattering angle of 173° to determine the hydrodynamic diameter, polydispersity index (PDI), and zeta potential of the green-synthesized AgNPs. The particle size analysis revealed a Z-average value of 57.28 nm, confirming that the particles fall well within the definitive nanoparticle range of 1–100 nm [10]. This optimal dimensions demonstrates that green synthesis utilizing frangipani leaf extract successfully yields AgNPs tailored for sensor applications, where nanoparticle size critically dictates optical properties and surface reactivity [37]. Furthermore, the uniformity of the formulation was assessed via its PDI. While a PDI value exceeding 0.5 typically signifies a broad and heterogeneous size distribution [38, 39], the AgNPs in this study exhibited a narrow PDI of 0.3254, indicating a highly homogeneous and uniform particle size distribution [40]. Crucially, the nanoparticles demonstrated good electrostatic stability, characterized by a zeta potential of -25.53 mV. This significant negative charge falls firmly within the stable category, providing sufficient interparticle repulsive forces to effectively inhibit aggregation and ensure long-term colloidal stability [31, 34].

Table 1. Particle size distribution, polydispersity index (PDI), and zeta potential of green-synthesized AgNPs

Extract concentration (%)	Z-Average (nm)	Polydispersity Index (PDI)	Zeta Potential (mV)
0.5%	57.28 ± 0.475	0.3254 ± 0.0051	-25.53 ± 0.4423

Crystal Structure Analysis (XRD)

The crystalline structure of the green-synthesized AgNPs was investigated using X-ray diffraction (XRD) on a Bruker D8 Advance diffractometer equipped with Cu Kα radiation (λ = 0.15406 nm), operated at 40 kV and 40 mA. Diffraction data were collected over a 2θ range of 20°–90° with a step size of 0.02°. The XRD pattern (Figure 4) confirmed the successful formation of crystalline AgNPs with a face-centered cubic (FCC) structure. Three prominent diffraction peaks were observed at 29.318°, 37.937°, and 61.958°, with the most intense peak located at 37.937°, corresponding to the (111) crystallographic plane of metallic silver. This peak is in close agreement with the standard silver diffraction peak at 38.11° reported in JCPDS No. 04-0783, confirming the formation of AgNPs. The predominance of the (111) plane is characteristic of silver nanoparticles due to its highly stable, densely packed atomic arrangement, which is the energetically favored crystal orientation [41]. The diffraction peak at 61.958° further supports the presence of crystalline silver. However, a slight shift from the standard position was observed, possibly attributable to the nanoscale particle size and associated lattice strain. In addition,

the appearance of a diffraction peak at 29.318° is likely associated with residual organic compounds or biomolecules from the frangipani leaf extract adsorbed on the nanoparticle surface, indicating their role as reducing and stabilizing agents during the biosynthesis process [42]. Similar observations have been reported for green-synthesized AgNPs produced using *Aspergillus terreus*, where additional diffraction peaks were attributed to organic functional groups involved in nanoparticle reduction and stabilization [43]. Notably, the characteristic silver reflections corresponding to the (200) and (311) planes at approximately 44.3° and 77.4°, respectively, were absent or significantly suppressed. This phenomenon may result from preferential crystal growth along the (111) orientation, combined with the influence of the organic capping layer, which induces nanoscale confinement and broadens diffraction peaks [44]. Consequently, the relative intensities of weaker reflections may decrease below the instrumental detection limit, a synthesis-induced texture effect widely reported for noble metal nanoparticles synthesized via green routes [45,46].

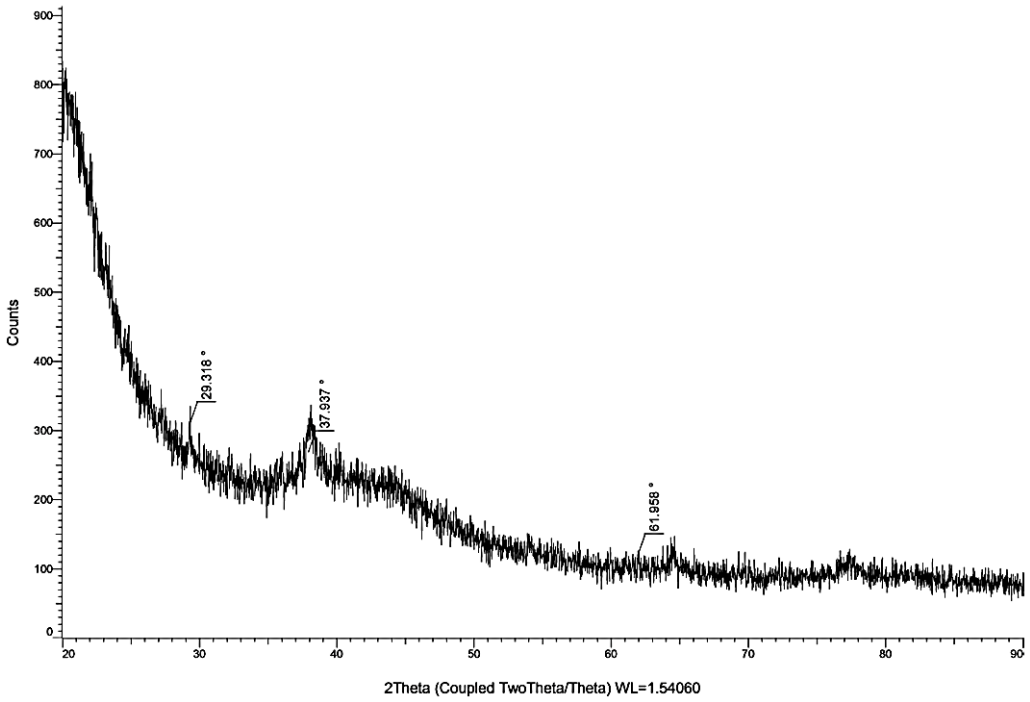

Figure 4. XRD diffractogram of AgNPs synthesized using Plumeria acuminata L. leaf waste extract showing the characteristic diffraction peaks at (111) and (220).

Based on Table 2, the d-spacing value of the main peak of 2.36981 Å is close to the standard value of the (111) silver plane, which is 2.359 Å, thus indicating the suitability of the crystal structure of the AgNPs formed. The broadened diffraction pattern (peak broadening) also indicates that the particle size is on the nanoscale. The broadening of the XRD peak is related to the small crystallite size, where the smaller the crystallite size, the wider the diffraction peak will be [47]. The crystallite size is calculated using the Debye-Scherrer equation:

$$D = \frac{K\lambda}{\beta \cos \theta}$$

where D is the crystallite size, k is the Scherrer constant, λ is the X-ray wavelength, β is the FWHM value in radians, and θ is the Bragg angle. Based on the FWHM value of the main peak of 0.399°, the crystallite size is 21.98 nm. This value indicates that the particles formed are in the nanoparticle range [47].

The synthesized silver nanoparticles exhibited an average crystallite size of 21.98 nm, as estimated from the XRD diffraction pattern using the Scherrer equation. This value specifically represents the size of the coherently diffracting crystalline domains within the nanoparticle structure [48]. In contrast, particle size analysis (PSA) revealed a significantly larger average diameter of 57.28 nm. This discrepancy is inherently tied to the distinct physical principles underlying each characterization technique. While XRD measures the internal crystalline core via diffraction peak broadening, PSA determines the hydrodynamic

diameter of nanoparticles dispersed in a liquid medium [49]. Consequently, the PSA measurement encompasses the metallic silver core along with its solvation shell, including adsorbed solvent molecules, potential weak agglomerates, and the layer of plant-derived phytochemical capping agents (such as secondary metabolites). These surface-bound biomolecules expand the effective particle diameter in solution. Therefore, the observation that the PSA-derived particle size exceeds the XRD crystallite size is consistent with established nanoparticle characterization principles, confirming successful capping and stabilization of the nanoparticles by the plant extract's bioactive constituents.

Table 2. XRD peak characteristics and crystallite size analysis of AgNPs synthesized using *Plumeria acuminata* L. leaf extract.

Peak	2θ (°)	d-spacing (Å)	Relative Intensity (%)	FWHM (°)	Possible Plane (hkl)
1	29.318	3.04385	100.0	0.100	–
2	37.937	2.36981	89.4	0.399	(111)
3	61.958	1.49653	55.7	0.247	(220)

Selectivity Study of AgNPs Toward Metals Ion

A selectivity test was conducted to evaluate the ability of AgNPs to detect Pb^{2+} ions compared to other metal ions, namely Na^{+}, Ca^{2+}, K^{+}, Zn^{2+}, and Mg^{2+}. Based on the UV-Vis spectrum results in Figure 5, it can be seen that the addition of Pb^{2+} ions resulted in the most significant change in absorbance intensity compared to the other ions. In this study, the specific maximum wavelength of AgNPs-Pb was 439 nm, while the maximum wavelength of AgNPs was 408 nm. This shift in the maximum wavelength of AgNPs indicates an interaction between AgNPs and Pb^{2+} ions. The absorbance ratio data, with Pb^{2+} ions showing the highest value compared to other metal ions, indicate a stronger interaction between Pb^{2+} ions and AgNPs.

This interaction generally occurs through the adsorption of metal ions on the nanoparticle surface, which can trigger changes in surface conditions, thus influencing the surface plasmon resonance (SPR) phenomenon. These changes can include an increase or decrease in absorbance intensity or a shift in the maximum wavelength. This phenomenon has been widely reported in previous studies, indicating that the interaction between metal ions and metal nanoparticles can cause changes in optical characteristics due to changes in electron distribution on the nanoparticle surface [50].

According to Figure 6, the visual observation results also support the spectrophotometric data, where solutions containing Pb^{2+} exhibit a more pronounced color change than those containing other ions. This color change is related to the surface plasmon resonance (SPR) phenomenon, which is sensitive to changes in the nanoparticle's environmental conditions. Certain metal ions can cause nanoparticle aggregation, resulting in a color change from yellow to darker or varying intensity. This aligns with research suggesting that nanoparticle aggregation can cause significant color changes due to changes in interparticle spacing, thus affecting optical properties and enabling visual detection of target analytes [51].

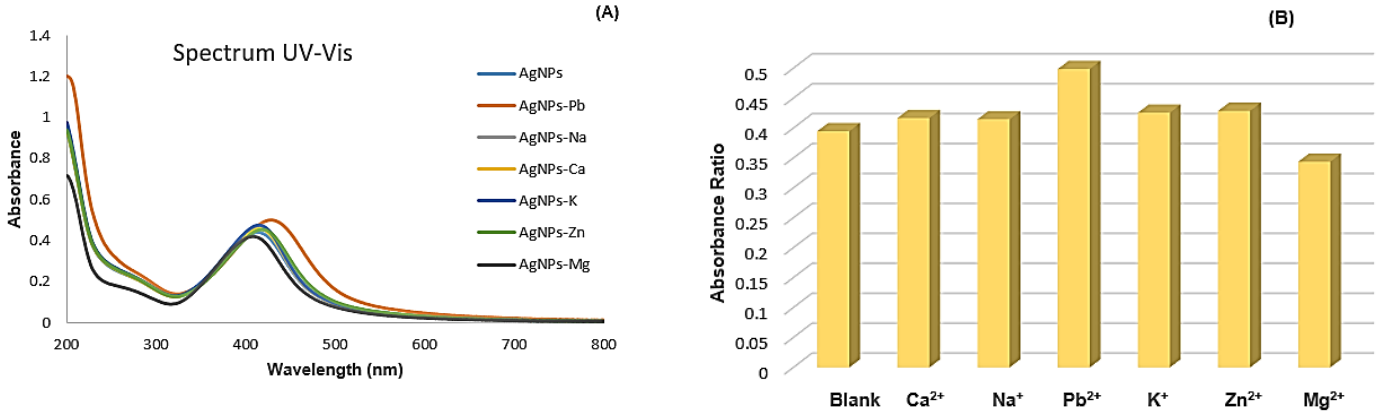

Figure 5. Selectivity study of green-synthesized AgNPs toward Pb^{2+}, Na^{+}, Ca^{2+}, K^{+}, Zn^{2+}, Mg^{2+} ions based on UV–Vis spectra (A) and absorbance ratio (B)

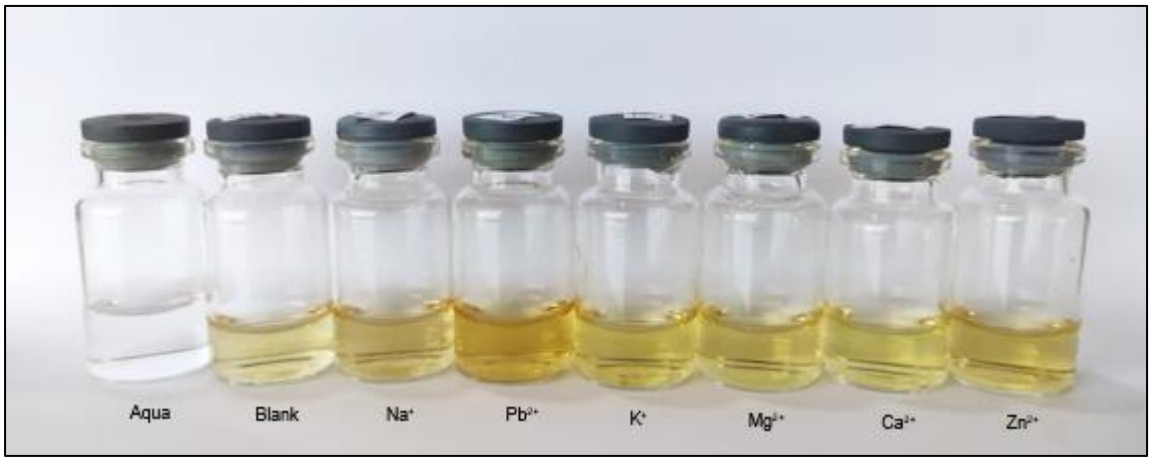

Figure 6 Visual color changes of AgNP solutions in the presence of different ions (Na^+, Pb^{2+}, K^+, Mg^{2+}, Ca^{2+}, and Zn^{2+}).

Analytical Performance of AgNPs as Pb Sensor

Analytical performance testing was conducted to evaluate the ability of green-synthesized AgNPs using frangipani leaf waste extract as a biosensor in detecting Pb^{2+} ions. Evaluation was carried out through observing visual changes, measuring absorbance responses using a UV-Vis spectrophotometer, and method validation parameters, including linearity, limit of detection (LOD), limit of quantification (LOQ), precision, and accuracy. Good analytical performance indicates that AgNPs are able to provide a sensitive and consistent response to changes in Pb^{2+} ion concentration. Figure 7 shows the visual changes of AgNPs after the addition of Pb^{2+} ions at various standard concentrations. The blank solution without the addition of Pb^{2+} has an intense yellow color compared to the addition of Pb^{2+}. As the Pb^{2+} concentration increases, the color of the solution appears paler, where the color change indicates an interaction between Pb^{2+} ions and the AgNPs surface, which affects the surface plasmon resonance (SPR) phenomenon [52]. The visual changes in Figure 7 are in line with the results of the calibration curve in Figure 8. Based on the results of linear regression, the equation is obtained:

$$y = -0.0034x + 0.5377$$

With a coefficient of determination (R^2) of 0.9922 and a correlation coefficient (r) of -0.9961, which is close to 1, indicating a good linear relationship between Pb^{2+} concentration and the absorbance response of AgNPs [26].

The negative slope value in the regression equation indicates that increasing Pb^{2+} concentration causes a decrease in the absorbance value of AgNPs. These results are consistent with the visual changes in the solution, which appear paler at higher Pb^{2+} concentrations. The higher the Pb^{2+} concentration, the greater the interaction of metal ions with the AgNPs surface, resulting in a decrease in the intensity of the characteristic AgNPs color and a decrease in UV–Vis absorbance [53]. This decrease in absorbance is thought to occur due to changes in the surface condition of the nanoparticles after interacting with Pb^{2+} ions, which weakens the SPR intensity. This interaction can affect the electron distribution on the AgNPs' surface, thus decreasing the nanoparticles' ability to absorb light. Therefore, the negative linear relationship obtained in the calibration curve still indicates a good sensor response because the change in absorbance occurs consistently with increasing Pb^{2+} concentration [54]. All subsequent absorbance values for the calibration curve and real sample matrices were recorded at the complexed localized surface plasmon resonance (LSPR) peak of λ_{max} 439 nm.

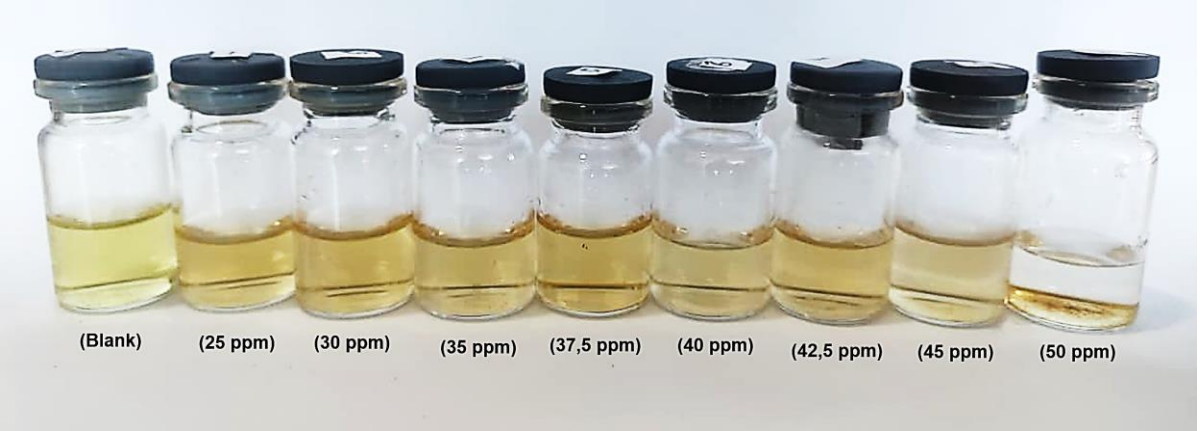

Figure 7. Visual observation of AgNPs response toward increasing Pb^{2+} concentrations, where the first vial represents the blank AgNPs solution without Pb^{2+}

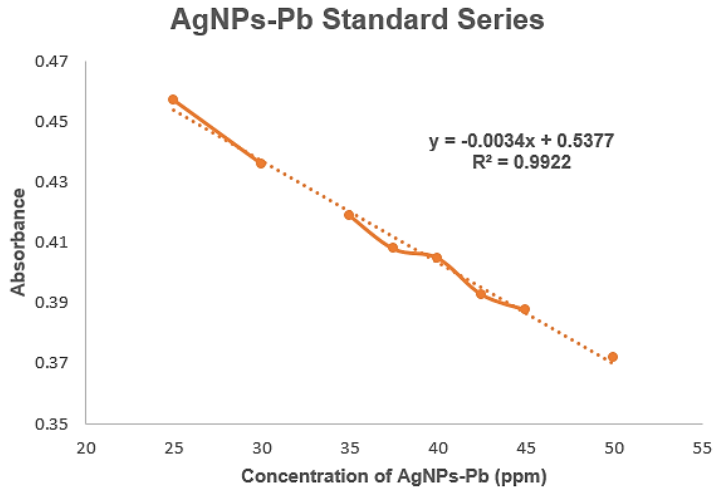

Figure 8. Calibration curve of AgNPs toward Pb^{2+} detection based on UV–Vis absorbance response

Table 3. Validation parameters of AgNPs-based colorimetric sensor for Pb^{2+} detection

Parameter	Result
Regression equation	y = −0.0034x + 0.5377
Linearity range	25–50 ppm
r	-0.9961
R^2	0.9922
LOD	3.17 ppm
LOQ	9.59 ppm
Precision (%RSD)	3.01%
Accuracy (%Recovery)	98.69–107.03%

The method validation results in Table 3 show that AgNPs have good performance as a Pb^{2+} ion biosensor for the limit of detection (LOD) value obtained at 3.17 ppm and the limit of quantification (LOQ) obtained at 9.59 ppm, indicating that AgNPs are able to detect Pb^{2+} ions at low concentrations. Precision testing shows a %RSD value of 3.01%, which means this method has adequate repeatability. Based on ICH Q2(R1) guidelines, an analytical method is considered sufficiently precise if the %RSD value does not exceed 5%. In addition, the accuracy test provides recovery results in the range of 98.69–107.03%,

which still meets the acceptance limits for analytical methods. Recovery close to 100% indicates that AgNPs can be used to detect Pb^{2+} ions with relatively small measurement errors [26].

To adequately position the analytical capability of the proposed AgNPs sensor within the wider landscape of green nanotechnology, its performance metrics were benchmarking against several state of the art green-synthesized AgNPs sensors reported in recent literature (Table 4.).

Table 4. Analytical performance comparison of various green-synthesized AgNPs colorimetric sensors for heavy metal ions

Plant Source / Green Matrix	Target Metal Ion	Limit of Detection (LOD)	Reference
Orange Peel Waste	Pb^{2+}	0.0103 ppm	[55]
Coffee Grounds/ Coffee Peel	H_2O_2	1.26 mM	[56]
Acacia raddiana Leaves	Hg^{2+}, Cu^{2+}, Pb^{2+}, Co^{2+}	1.63×10^{-5} M (~3.38 ppm for Pb^{2+})	[57]
Mussel-Inspired Protein (polyDOPA)	Pb^{2+}, Cu^{2+}	9.4×10^{-5} M (~19.47 ppm for Pb^{2+})	[58]
L-Tyrosine Biomolecule	Hg^{2+}, Mn^{2+}, Pb^{2+}	16 nM (~0.0033 ppm for Pb^{2+} via AuNPs)	[59]
Present Work	Pb^{2+}	3.17 ppm (1.53×10^{-5} M)	This Study

As evaluated from the comparative data, the green synthesis strategy implemented in this work yields an AgNPs platform with an LOD of 3.17 ppm for Pb^{2+} ions. This value is notably superior to several classical biogenic protocols, such as those relying on *Acacia raddiana* (3.38 ppm) and polyDOPA protein-stabilized matrices (19.47 ppm). While alternative amino-acid or chemical-hybrid frameworks achieve lower analytical trace values, current approach circumvents complex multi-component processing and specialized sunlight irradiation dependencies. Consequently, it establishes a highly straightforward, low-cost, eco-friendly indicator.

Detection of Pb in Lipstick Sample

Testing the application of AgNPs to lipstick samples was conducted to evaluate the biosensor's ability to detect Pb^{2+} ions in real cosmetic samples. In Figure 9, the lipstick sample was prepared through a digestion process with aqua regia (HNO_3:HCl (1:3)). During the heating process, the solution produced brown smoke, indicating the oxidation of organic compounds in the sample. Heating was continued until the brown smoke disappeared to ensure the digestion process was successful and the metal ions in the sample were dissolved [60]. The solution was cooled and filtered to obtain a clear filtrate, then diluted and neutralized with demineralized water and 1.0 N NaOH to a pH of 6-7 before reacting with the AgNPs. The neutralization process was carried out to reduce the acidity of the solution to prevent it from affecting the stability of the AgNPs during the detection process. The AgNPs and sample mixture were incubated at 50°C for 10 minutes before being analyzed using a UV–Vis spectrophotometer at a maximum wavelength of 439 nm.

UV-Vis spectrophotometric analysis of the lipstick samples treated with the AgNPs biosensor revealed an absence of the characteristic 439 nm maximum wavelength across all samples. This aligns with visual observations, which failed to exhibit the typical color transitions observed in the AgNPs-Pb standard solutions (Figure 10). While the standard series exhibited a clear concentration-dependent color change and a corresponding shift in absorbance with increasing Pb^{2+} concentrations [61], the lipstick samples showed no such colorimetric response under these experimental conditions. Consequently, it can be concluded that the concentration of Pb^{2+} in the analyzed lipstick samples remains below the Limit of Detection (LOD) of the developed biosensor

To confirm the ability of AgNPs to detect Pb^{2+} in cosmetic matrices, one of the samples was used as an artificial sample by adding a standard Pb^{2+} solution to a theoretical concentration of 25 ppm [62]. After the addition of Pb^{2+}, the solution exhibited a visual response change, as seen in Figure 10, where the artificial sample resembled the standard AgNPs-Pb solution at the same concentration. This change indicates that AgNPs are capable of providing a colorimetric response to the presence of Pb^{2+} ions even within the cosmetic sample matrix.

UV–Vis measurements showed that the artificial sample had an absorbance value in the range of 0.452–0.455 at a wavelength of 439 nm. Based on the linear regression equation, the calculated Pb^{2+} concentrations were 24.32; 24.91; and 25.20 ppm, respectively. These values are close to the theoretical concentration of 25 ppm added to the sample. Furthermore, a recovery value of 99.25% and a precision

(%RSD) of 1.81% were obtained. A recovery value approaching 100% indicates good method accuracy, while a low %RSD value indicates good method repeatability in the lipstick sample matrix [26].

The strong agreement among the visual colorimetric response, absorbance measurements, and calculated concentrations from synthetic samples clearly demonstrates the ability of the green-synthesized AgNPs to effectively detect Pb^{2+} in cosmetic matrices. This consistency across analytical parameters confirms the reliability of the developed colorimetric sensing system and validates the interpretation of the lipstick sample analysis. Notably, the absence of visual changes or absorbance variations in the tested lipstick samples indicates that the Pb^{2+} concentration if present fell below the sensor's limit of detection (LOD) under the applied experimental conditions. Given the method's LOD of 3.17 ppm, trace levels of Pb^{2+} below this threshold would remain undetected by the biosensor. Consequently, further research comparing the AgNPs biosensor against standard reference methods, such as atomic absorption spectroscopy (AAS) or inductively coupled plasma mass spectrometry (ICP-MS), is necessary to rigorously evaluate its performance, accuracy, and reliability in real world cosmetic analysis.

Nevertheless, several factors should be considered when applying this sensing platform to complex cosmetic formulations. Mineral pigments, particularly iron oxides, are commonly used as colorants in cosmetic products and constitute an important component of many formulations [63]. The presence of free Fe^{3+} ions may interfere with the sensing mechanism of the AgNPs biosensor, potentially affecting its selectivity and analytical performance. Therefore, future studies should include comprehensive selectivity assessments against Fe^{3+} ions to further validate sensor specificity. In addition, potential matrix effects associated with chloride-containing ingredients should be carefully evaluated, as chloride ions may induce AgCl formation and consequently influence nanoparticle stability. Excess halides can promote chemical erosion or phase transformation of AgNPs, thereby affecting sensor sensitivity and reliability [64].

Figure 9. Preparation and digestion process of lipstick samples using aqua regia prior to Pb^{2+} analysis

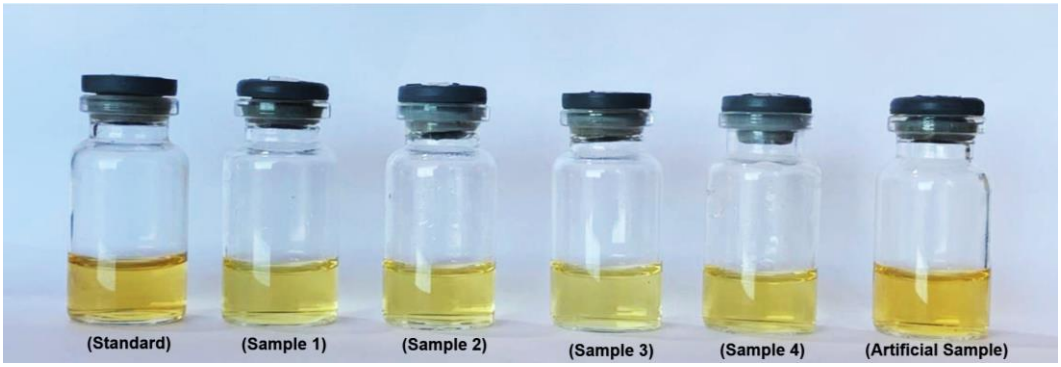

Figure 10. Visual appearance of AgNPs after reaction with Pb^{2+} standard solution, lipstick samples, and artificial sample used for Pb^{2+} detection.

Conclusions

The synthesis of AgNPs was successfully carried out using waste frangipani (*Plumeria acuminata* L.) leaf extract using the green synthesis method. The formation of AgNPs was indicated by a change in the solution color and the appearance of an SPR absorption peak at a wavelength of 408 nm in UV–Vis analysis. XRD characterization results also showed that the formed AgNPs have a face-centered cubic (FCC) crystal structure with a dominant (111) crystal plane and a crystallite size of 21.98 nm. Selectivity test results indicated that AgNPs respond better to Pb^{2+} ions than other metal ions, thus making them potentially useful as a colorimetric sensor for Pb^{2+} detection. Analytical performance evaluation demonstrated good linearity with an R^2 value of 0.9922, and accuracy and precision values that meet method validation criteria. The obtained LOD and LOQ values also indicated that the method has sufficient sensitivity for Pb^{2+} analysis.

When testing the lipstick samples, no visual response or absorbance was detected that matched the Pb^{2+} standard solution, suggesting that any existing lead concentrations fell below the method's limit of detection under the current experimental conditions. Conversely, spiked samples containing the Pb^{2+} standard yielded distinct visual responses and concentration values closely aligned with theoretical amounts, confirming that the green-synthesized AgNPs can successfully detect Pb^{2+} within complex cosmetic matrices. Ultimately, while AgNPs demonstrate promising potential for colorimetric Pb^{2+} detection in cosmetics, further rigorous validation using a larger sample cohort and established analytical techniques such as ICP-MS or AAS is warranted.

Conflicts of Interest

The authors declare that there is no conflict of interest regarding the publication of this paper.

Acknowledgment

In this study, we would like to thank PT DKSH, especially Mrs. Wiji Rahayu, who helped with the particle size analyzer analysis.

References

[1] Jităreanu, A., Trifan, A., Caba, I. C., Mârțu, I., and Agoroaei, L. (2025). An Overview of Heavy Metals in Cosmetic Products and Their Toxicological Impact. *Appl. Sci.*, *15(24)*, 1–42, doi: 10.3390/app152412883

[2] BPOM, "Kepala BPOM Rilis Daftar Kosmetik Mengandung Bahan Berbahaya dan atau Dilarang Hasil Intensifikasi Pengawasan di Awal Tahun 2025," *Badan Pengawas Obat dan Makanan Indones.*, no. April, p. Nomor HM.01.1.2.04.25.100 Tanggal 22 April 2025, 2025, [Online]. Available: https://www.pom.go.id/siaran-pers/kepala-bpom-rilis-daftar-kosmetik-mengandung-bahan-berbahaya-dan-atau-dilarang-hasil-intensifikasi-pengawasan-di-awal-tahun-2025

[3] Saah, S. A., Boadi, N. O., Sakyi, P. O., and Smith, E. Q. (2024). Human health risks of lead, cadmium, and other heavy metals in lipsticks. *Heliyon*, *10(23),* p. e40576, doi: 10.1016/j.heliyon.2024.e40576

[4] Anis, I. (2020). Biofarmasetikal Tropis Biofarmasetikal Tropis. *Trop. J. Biopharm.*, 2(2), 158–169

[5] Arifiyana, D. (2018). Identifikasi Cemaran Logam Berat Timbal (Pb) pada Lipstik yang Beredar di Pasar Darmo Trade Center (DTC) Surabaya dengan Reagen Sederhana. *Journal Pharm. Sci.*, *3(1),* 13–16 doi: 10.53342/pharmasci.v3i1.68

[6] Raj, K., and Das, A. P. (2023). Lead pollution: Impact on environment and human health and approach for a sustainable solution. *Environ. Chem. Ecotoxicol.*, 5, 79–85, doi: 10.1016/j.enceco.2023.02.001

[7] World Health Organization, "Lead poisoning," 2024. [Online]. Available: https://www.who.int/news-room/fact-sheets/detail/lead-poisoning-and-health

[8] Jin, M., Yuan, H., Liu, B., Peng, J., Xu, L., and Yang, D. (2020). Review of the distribution and detection methods of heavy metals in the environment. *Anal. Methods*, *12(48),* 5747–5766, doi: 10.1039/d0ay01577f.

[9] Nuttall, K. L., Gordon, W. H., and Ash, K. O. (1995). Inductively coupled plasma mass spectrometry for trace element analysis in the clinical laboratory. *Ann. Clin. Lab. Sci.*, *25(3)*, 264–271

[10] Ibrahim, N. H., Taha, G. M., Hagaggi, N. S. A., and Moghazy, M. A. (2024). Green synthesis of silver nanoparticles and its environmental sensor ability to some heavy metals. *BMC Chem.*, *18(1)*, 1–34, doi: 10.1186/s13065-023-01105-y

[11] Khan, S. R., Sharma, B., Chawla, P. A., and Bhatia, R. (2022). Inductively Coupled Plasma Optical Emission Spectrometry (ICP-OES): a Powerful Analytical Technique for Elemental Analysis. *Food Anal. Methods*, *15(3)*, 666–688, doi: 10.1007/s12161-021-02148-4

[12] Sudarman, F., Shiddiq, M., Armynah, B., and Tahir, D. (2023). Silver nanoparticles (AgNPs) synthesis methods as heavy-metal sensors: a review. *Int. J. Environ. Sci. Technol.*, *20(8)*, 9351–9368, doi: 10.1007/s13762-022-

04745-0
[13] Roy, A., Datta, S., Luthra, R., Khan, M. A., Gacem, A., Hasan, M. A., Yadav, K. K., Ahn, Y. and Jeon, B-H. (2022). Green synthesis of metalloid nanoparticles and its biological applications: A review. *Front. Chem,* 10, 994724, doi: 10.3389/fchem.2022.994724
[14] Nguyen, N. P. U., Dang, N. T., Doan, L., and Nguyen, T. T. H. (2023). Synthesis of Silver Nanoparticles: From Conventional to 'Modern' Methods—A Review. *Processes*, *11(9)*, doi: 10.3390/pr11092617
[15] Sujarwo, W., Caneva, G., and Zuccarello, V. (2020). Patterns of plant use in religious offerings in bali (Indonesia). *Acta Bot. Brasilica*, *34*(1), 40–53, https://doi.org/10.1590/0102-33062019abb0110
[16] Widiyaningtiyas, M. I., Putra, R. A., Ekawati, E. R., Herawati, D. and Mustika, A. (2025). The Effect of a Combination of Ethanol Extract from Leaves and Flowers of Plumeria acuminata L. Against Aedes aegypti Larvae. *J. Multidiscip. Appl. Nat. Sci.*, *5*(1), 18–31, https://doi.org/10.47352/jmans.2774-3047.225
[17] Sari, N. K. Y., Sintia, P. L., Deswiniyanti, N. W., Permatasari, A. A. A. P. (2023). Aktivitas Antimikroba Infusa Dan Ekstrak Bunga Kamboja Putih (*Plumeria acuminata*) Secara *In Vitro*. *Jurnal Kesehatan Terpadu, 7*(1), 19–24
[18] Widiyaningtiyas, M. I., Putra, R. A., Ekawati, E. R., Herawati, D., Mustika, A. (2024). The effect of a combination of ethanol extract from leaves and flowers of *Plumeria acuminata* L. against *Aedes aegypti* larvae. *Journal of Multidisciplinary Applied Natural Science*, *5*(1), 18–31. https://doi.org/10.47352/jmans.2774-3047.225
[19] Dube, E., Juanga-Labayen, J. P., Labayen, M. (2024). From plant metabolites to functional nanomaterials: Advances in phytochemical-mediated silver nanoparticle synthesis and applications. *Chemistry*, *6*(2), 40–62. https://doi.org/10.3390/chemistry6020040
[20] Kafesa, A. (2024). Fundamentals of the nanosilver reaction in green synthesis. *IntechOpen.* https://doi.org/10.5772/intechopen.1240238
[21] Omer Abdulazeez, T., Alrasheid, A. A., Kabbashi, A. S., and Ayoub, S. M. H. (2023). Green Synthesis of Silver Nanoparticles from Psidium guajava Leaf Extract: Characterization and Evaluation of Antibacterial Activity Against Common Pathogens. *Am. J. Nano Res. Appl.*, *11*(2), 19–25, 2023, https://doi.org/10.11648/j.nano.20231102.11
[22] Zannotti, M., Piras, S., Rita, L., Biesuz, R., and Giovannetti, R. (2024). Spectrochimica Acta Part A : Molecular and Biomolecular Spectroscopy Silver nanoparticles from orange peel extract : Colorimetric detection of Pb^{2+} and Cd^{2+} ions with a chemometric approach. *Spectrochim. Acta Part A Mol. Biomol. Spectrosc, 323*, 124881, https://doi.org/10.1016/j.saa.2024.124881
[23] Sulistyarti, H., Mashuri, M., Ari, U., Fadhila, M., and Cahyaningrum, A. (2022). Green synthesis of silver nanoparticles using Coffea canephora fruit skin extract and its application for mercury detection in face cream samples. *Anal. Sci.*, *39*(3), 335–346, https://doi.org/10.1007/s44211-022-00237-w.
[24] Sevinc-Sasmaz, C., Erci, F., Torlak, E., and Yöntem, M. (2025). Characterization of Silver Nanoparticles Synthesized Using Hypericum perforatum L. and Their Effects on Staphylococcus aureus. *Microsc. Res. Tech.*, *88*(8),. 2321–2332, https://doi.org/10.1002/jemt.24862
[25] Erliyanti, R. P. N. K., Wira, G. R., Maharani, H. P., Pujiastuti, C. (2025). Biosynthesis of Silver Nanoparticles Using Black Pepper (*Piper nigrum* L.) Essential Oil as a Bioreductor. *Jurnal Rekayasa Kimia & Lingkungan*, *20*(1), 112–125.
[26] International Conference on Harmonisation (ICH), "Validation of Analytical Procedures: Text and Methodology Q2(R1)," 2005.
[27] Eker, F., Akdaşçi, E., Duman, H., Bechelany, M., and Karav, S. (2025). Green Synthesis of Silver Nanoparticles Using Plant Extracts: A Comprehensive Review of Physicochemical Properties and Multifunctional Applications. *Int. J. Mol. Sci.*, *26*(13), 1–50, https://doi.org/10.3390/ijms26136222.
[28] Widiyaningtiyas, M. I., Putra, R. A., Ekawati, E. R., Herawati, D., and Mustika, A. (2025). The effect of a combination of ethanol extract from leaves and flowers of *Plumeria acuminate* L. against *Aedes aegypti* larvae. *Journal of Multidisciplinary Applied Natural Science*, *5*(1), 168–176
[29] Barleany, D. R., Saleh, A. I., and Pitaloka, A. B. (2025). Green Synthesis of Silver Nanoparticles Using Caulerpa racemosa Extract as Bioreductor : Characterization and Antibacterial Activity. *J. Rekayasa Kim. Lingkung.*, *20*(2), 250–260, https://doi.org/10.23955/rkl.v20i2.276.
[30] Lestari, G. A. D., Kempen, N. W. N. K. V., Cahyadi, K. D., Esati, N.K. (2024). Penggunaan Bioreduktor Ekstrak Air Daun Sirsak (*Annona mucirata* L.) Untuk Fitosintesis Nanopartikel Perak (Npag) Dengan Berbagai Variasi Rasio Campuran. *Inovasi Teknik Kimia, 9(3)*, 169-176
[31] Gupta, P., Ilyas, H., Raghav, D. S., and Tomar, S. (2025). "Sustainable synthesis of silver nanoparticles via hordeum vulgare seed extract : catalysis , antioxidant , anti-cancerous and antimicrobial potential. *Discov. Mater.*, *5,* https://doi.org/10.1007/s43939-025-00342-3.
[32] Negri, C., Colombo, R., Bracconi, M., Atzori, C., and Donazzi, A. (2024). "Operando UV-vis spectroscopy for real-time monitoring of nanoparticle size in reaction conditions: a case study on rWGS over Au nanoparticles. *Catal. Sci. Technol.*, 1318–1327, https://doi.org/10.1039/d3cy01392h.
[33] Iravani, S., Korbekandi, H., Mirmohammadi, S. V., and Zolfaghari, B. (2013). Synthesis of silver nanoparticles : chemical , physical and biological methods. *Res. Pharm. Sci.*, *9*, 385–406.
[34] Baran, A., Ghorbanzadeh, V., Doğan, Y., Ahmadian, E., and Zulfugarova, P. (2026). "Green synthesis of silver nanoparticles from Elaeagnus angustifolia extract : characterization and evaluation of antibacterial and cytotoxic properties. *Discov. Nano*, https://doi.org/10.1186/s11671-025-04423-3.
[35] Shejawal, K. P., Randive, D. S., Bhinge, S. D., Bhutkar, M. A., Wadkar, G. H., and Jadhav, N. R. (2020). Green synthesis of silver and iron nanoparticles of isolated proanthocyanidin : its characterization , antioxidant , antimicrobial , and cytotoxic activities against COLO320DM and HT29. *J. Genet. Eng. Biotechnol.*, *18*(1), 43, https://doi.org/10.1186/s43141-020-00058-2.
[36] Zhang, X., Liu, Z., Shen, W., and Gurunathan, S. (2016). Silver Nanoparticles : Synthesis , Characterization , Properties, Applications, and Therapeutic Approaches. *Int. J. Mol. Sci. Rev.*, https://doi.org/10.3390/ijms17091534.
[37] Abbas, R., Luo, J., Qi, X., Naz, A., Khan, I. A., Liu, H., Yu, S., Wei, J. (2024). Silver Nanoparticles: Synthesis,

Structure, Properties and Applications. *Nanomaterials*, *14*(17), 1425. https://doi.org/10.3390/nano14171425
[38] John, R., Monpara, J., Swaminathan, S., and Kalhapure, R. (2024). Chemistry and Art of Developing Lipid Nanoparticles for Biologics Delivery : Focus on Development and Scale-Up. *Pharmaceutics*, https://doi.org/10.3390/pharmaceutics16010131.
[39] Udepurkar, A. P., Mampaey, L., Clasen, C., and Kuhn, S. (2024). Reaction Chemistry & Engineering enabled by an ultrasonic microreactor. 2208–2217, https://doi.org/10.1039/d4re00107a.
[40] Viana, T. (2022). Redispersible 3D printed nanomedicines : An original application of the semisolid extrusion technique. *Int. J. Pharm.*, *624*, 122029, https://doi.org/10.1016/j.ijpharm.2022.122029.
[41] Patriciaa, A. G. J. (2022). An Investigation of Novel Nano Material Silver Nano Dots Synthesis and Characterization Using Simple Sugar Fructose. *J. Mater. Sci. Eng.*, *11*, 4–7, https://doi.org/10.37421/ 2169-0022.2022.11.12.
[42] Roopan, S. M., Madhumitha, G., Rahuman, A. A., Kamaraj, C., Bharathi, A., & Surendra, T. V. (2013). Low-cost and eco-friendly phyto-synthesis of silver nanoparticles using *Cocos nucifera* coir, characterization and larvicidal activity. *Industrial Crops and Products*, *43*, 631-635, https://doi.org/10.1016/j.indcrop.2012.08.004
[43] Lotfy, W. A., Alkersh, B. M., Sabry, S. A., Ghozlan, H. A., and Castro, G. R. (2021). Biosynthesis of Silver Nanoparticles by Aspergillus terreus : Characterization , Optimization, and Biological Activities. *Front. Bioeng. Biotechnol.*, *9*, https://doi.org/10.3389/fbioe.2021.633468.
[44] Asif, M., Yasmin, R., Asif, R., Ambreen, A., Mustafa, M., & Umbreen, S. (2022). Green synthesis of silver nanoparticles (AgNPs), structural characterization, and their antibacterial potential. *Dose-Response*, *20*(2), https://doi.org/10.1177/15593258221088709
[45] Kurra, H., Velidandi, A., Sarvepalli, M., Pabbathi, N. P. P., & Godishala, V. (2025). Aqueous Cymbopogon citratus extract mediated silver nanoparticles: Part I. Influence of synthesis parameters, characterization, and biomedical studies. *Nanomaterials*, *15*(5), 328, https://doi.org/10.3390/nano15050328
[46] Tamanna, N. J., Hossain, M. S., Bahadur, N. M., Ahmed, S. (2026). Green synthesis and characterization of silver (Ag) nanoparticles: Crystallographic analysis from X-ray diffraction. *Chemistry of Inorganic Materials*, *8*, 100144, https://doi.org/10.1016/j.cinorg.2026.100144
[47] Ojha, I. (2025). Plant mediated synthesis of silver nanoparticles using Alcea rosea leaf aqueous extract and evaluation of the biological activities. *Sci. Rep.*, *16*, 1–22, https://doi.org/10.1038/s41598-026-37480-4.
[48] Ali, A., Chiang, Y. W., & Santos, R. M. (2022). X-ray Diffraction Techniques for Mineral Characterization: A Review for Engineers of the Fundamentals, Applications, and Research Directions. *Minerals*, *12*(2), 205, https://doi.org/10.3390/min12020205
[49] Syarifah, S., Imawan, C., Handayani, W., & Djuhana, D. (2018). Biosynthesis of ferric oxide nanoparticles using Pometia pinnata J.R.Frost. & G.Forst. leaves water extract. *AIP Conference Proceedings*, *2024*(1). https://doi.org/10.1063/1.5064051
[50] Kelly, K. L., Coronado, E., Zhao, L. L., and Schatz, G. C. (2003). The Optical Properties of Metal Nanoparticles: The Influence of Size, Shape, and Dielectric Environment. *J. Phys. Chem. B*, *107*(3), 668–677, https://doi.org/10.1021/jp026731y.
[51] Vilela, D., González, M. C., and Escarpa, A. (2012). Sensing colorimetric approaches based on gold and silver nanoparticles aggregation : Chemical creativity behind the assay. A review. *Anal. Chim. Acta*, *751*, 24–43, https://doi.org/10.1016/j.aca.2012.08.043
[52] Kołątaj, K., Krajczewski, J., and Kudelski, A. (2020). Plasmonic nanoparticles for environmental analysis. *Environ. Chem. Lett.*, 529–542, https://doi.org/10.1007/s10311-019-00962-1.
[53] Choudhury, R., and Misra, T. K. (2018). Gluconate Stabilized Silver Nanoparticles as a Colorimetric Sensor for Pb^{2+}. *Colloids Surfaces A Physicochem. Eng. Asp.*, *545*, 179–187, https://doi.org/10.1016/j.colsurfa.2018.02.051.
[54] Almaquer, F. E. P., Ricacho, J. S. Y., and Ronquillo, R. L. G. (2019). Simple and rapid colorimetric sensing of Ni (II) ions in tap water based on aggregation of citrate-stabilized silver nanoparticles. *Sustain. Environ. Res.*, *29*, 1–10, https://doi.org/10.1186/s42834-019-0026-3.
[55] Zannotti, M., Piras, S., Remia, L., Appignanesi, D., Giovannetti, R. (2024). Selective ColorimetricDetection of Pb(II) Ions by Using Green Synthesized Gold Nanoparticles with Orange Peel Extract. *Chemosensors*, 12(33), https://doi.org/10.3390/chemosensors12030033
[56] Srikhao, N., Ounkaew, A., Kasemsiri, P., Theerakulpisut, S., Okhawilai, M., and Hiziroglu, S. (2022). Green synthesis of silver nanoparticles using the extract of spent coffee used for paper-based hydrogen peroxide sensing device. *Scientific Reports*, *12*(1). https://doi.org/10.1038/s41598-022-22067-6
[57] Ibrahim, N. H., Taha, G. M., Hagaggi, N. S. A., and Moghazy, M. A. (2024). Green synthesis of silver nanoparticles and its environmental sensor ability to some heavy metals. *BMC Chemistry*, *18*(1). https://doi.org/10.1186/s13065-023-01105-y
[58] Cheon, J., and Park, W. (2016). Green synthesis of silver nanoparticles stabilized with mussel-inspired protein and colorimetric sensing of lead(II) and copper(II) ions. *International Journal of Molecular Sciences*, *17*(12), 2006. https://doi.org/10.3390/ijms17122006
[59] Annadhasan, M., Muthukumarasamy, N., Senthil Kumar, P., and Rajendran, V. (2014). Green synthesized silver and gold nanoparticles for colorimetric detection of Hg^{2+}, Pb^{2+}, and Mn^{2+} in aqueous medium. *ACS Sustainable Chemistry & Engineering*, *2*(7), 1646–1655. https://doi.org/10.1021/sc400500z
[60] Berrow M. L., and Stein, W. M. (1983). Extraction of metals from soils and sewage sludges by refluxing with aqua regia. *Analyst*, *108(1283)*, 277–285, https://doi.org/10.1039/AN9830800277
[61] Desales, B., Duerme, K. I., Fundador, E. O. V., and Fundador, N. G. V. (2025). Colorimetric Detection of Pb^{2+} Using Green Synthesized AgNPs. *Solid State Phenom.*, 370, 17–21, https://doi.org/10.4028/p-d0maaD
[62] Thakur, D., Dubey, N. P., and Singh, R. (2024). A Review on Spike and Recovery Method in Analytical Method Development and Validation. *Crit. Rev. Anal. Chem.*, *54(7)*, 2053–2071, https://doi.org/10.1080/10408347.2022.2152275
[63] Kicińska, A., Kowalczyk, M. (2025). Health risks from heavy metals in cosmetic products available in the online consumer market. *Scientific Reports*, *15*, 11695611. https://doi.org/10.1038/s41598-024-83477-2

[64] Yuniarni, D. R., Aminah, Imawan, C. (2020). The effect of sodium chloride as a catalyst in the silver nanoparticles formation. *AIP Conference Proceedings*, *2314*(1), 020014. https://doi.org/10.1063/5.0035623